

## Thermal annealing of the torn vortex lattice in $\text{YBa}_2\text{Cu}_3\text{O}_7$ crystals

G. Pasquini\* and V. Bekkeris

Laboratorio de Bajas Temperaturas, Departamento de Física, Universidad de Buenos Aires, Pabellón 1, Ciudad Universitaria,  
Buenos Aires, Argentina

(Received 26 May 2004; revised manuscript received 4 November 2004; published 14 January 2005)

We report evidence that the ac driven solid vortex lattice in YBCO single crystals reorganizes and accesses to robust configurations with different effective pinning potential wells arising in response to different system histories. The curvature of the pinning wells was determined by measuring the real ac penetration depth in the linear regime with a sensitive ac susceptometer. The stability of the different static configurations without assistance of macroscopic forces was also investigated. We find that they have distinct characteristic relaxation times which may be related to elastic or plastic creep processes.

DOI: 10.1103/PhysRevB.71.014510

PACS number(s): 74.25.Qt, 74.72.Bk

### I. INTRODUCTION

Continuous efforts have been made in the past years to elucidate the complex dynamical behavior of the vortex lattice (VL) both in low- and high- $T_c$  superconductors.<sup>1,2</sup> More recently, much attention has been directed towards understanding driven lattices in the vicinity of the peak effect (PE) which refers to an anomalous nonmonotonous dependence of the critical current density  $J_c$  with both temperature and magnetic field.<sup>3</sup> Among the intriguing behaviors are the memory effects observed in low<sup>4,5</sup> and in high  $T_c$  materials (HTSC),<sup>6-9</sup> where the resistivity or the critical current density  $J_c$ , are found to be strongly dependent on the dynamical history of the VL.

A great amount of work was devoted to understand if this phenomenology is dominated by surface or bulk pinning properties. In  $\text{NbSe}_2$  (Ref. 5) and  $\text{BSCCO}$  (Ref. 10) samples, surface and geometrical barriers seem to play a fundamental role. In untwinned YBCO samples, vortex pinning at the sample surface has been reported to dominate over bulk pinning.<sup>11,12</sup> However, in materials with moderate anisotropy and high density of pinning centers, as is the case of well oxygenated twinned YBCO, transport properties at  $H_{dc} \gg H_{c1}$  are generally well described by bulk pinning forces. In particular, memory effects in the nonlinear ac regime in twinned YBCO crystals have been successfully described within a bulk critical state model.<sup>6,7,13</sup> We therefore consistently assume bulk pinning in what follows.

Characteristic of the observed driven dynamics is the increased mobility of the VL after assisting it with a temporarily symmetric (e.g., sinusoidal) ac field (or current).<sup>4,6,7,9</sup> A proposed mechanism<sup>14</sup> for the fast observed depinning in YBCO crystals, is the annealing of bulk magnetic gradients in a platelet placed in a perpendicular dc magnetic field by a weak *planar* ac magnetic field. A second invoked mechanism is an equilibration process assisted by the ac magnetic field.<sup>15</sup> The fluctuation energy produced in the sample under cyclic field variation would be a key element within this scenario.<sup>16</sup>

However, recent experiments in YBCO single crystals that cannot be accounted for within either of these two frameworks have been reported. We have shown<sup>7</sup> that a VL free from bulk field gradients assisted by an asymmetric ac field (e.g., sawtooth—although a small asymmetry is

enough) attains a vortex lattice configuration (VLC) and becomes less mobile. Moreover, mobility is also reduced if a temporarily symmetric ac field forces vortices into large excursions.<sup>17</sup> These striking features indicate that these effects have their origin in the oscillatory character of the vortex dynamics in YBCO crystals. Defects (e.g., dislocations), their creation or annihilation controlled by the different driven histories, might play a major role in the bulk VL response to an applied force.<sup>19</sup> A plausible picture is that the repeated interactions between vortex neighbors facilitates the healing of topological defects, while temporarily asymmetric ac fields or large vortex excursions promote their creation.<sup>20</sup>

An open issue that needs to be addressed is the connection between the attained mobility of the VL and the effective pinning potential wells. As was pointed out in Ref. 21, the effective or measured  $J_c$  in HTSC in the peak effect region is drastically affected by creep phenomena. Moreover, in typical nonlinear ac susceptibility experiments, vortices move changing the VL configuration. This led us to explore the VL near the static configuration acquired immediately after assisting it with a specific dynamical history. The solid VL in YBCO single crystals was prepared with different dynamical histories and explored using a very small ac field to measure ac susceptibility,<sup>22</sup> so vortices oscillate inside their effective pinning potential wells without modifying the configuration of the system. Results show that the oscillatory dynamical history not only determines the degree of mobility, but directly modifies the effective pinning potential wells: temporarily symmetric shaking reduces the curvature of the effective pinning wells and a larger curvature is recovered after shaking the VL with a temporarily asymmetric ac field of the same amplitude. Furthermore, the nature of these history dependent static VL configurations (VLCs) was investigated. Different warming-cooling protocols allowed us to analyze their degree of stability. We find very different characteristic decay times that probably involve distinct creep mechanisms.

This paper is organized as follows: In Sec. II we first describe the experimental array and the different experimental protocols that outline the dynamic history of the VL and then explain the numerical procedure followed to analyze the Campbell regime. Results and discussions are presented in Sec. III and conclusions are drawn in Sec. IV.

## II. METHODOLOGY

### A. Experiment

The samples used were  $\text{YBa}_2\text{Cu}_3\text{O}_7$  twinned single crystals<sup>18</sup> (typical dimensions  $0.6 \times 0.6 \times 0.02 \text{ nm}^3$ ) with  $T_c \sim 92 \text{ K}$  at zero dc field and  $\Delta T_c \sim 0.3 \text{ K}$  (10–90% criterion). Global ac susceptibility measurements were carried out with the usual mutual inductance technique. The measuring and the assisting ac field are provided by the primary coil and are parallel to the crystal  $c$  axis. The static magnetic field  $H_{dc}$  is provided by a magnet that can be rotated relative to the sample, and was oriented out of all the groups of twin planes.

The various VLCs were obtained following three protocols or dynamical histories. In the three cases, the sample is cooled in dc magnetic field avoiding bulk magnetic gradients, but each case differs in the applied assisting ac field. The first case is a dc field cool process without any assisting ac field (zero ac field cool, ZF<sub>ac</sub>C). A less mobile VLC,<sup>7</sup> that we call Asy, is obtained assisting the VL with an asymmetric (sawtooth) ac field (3.5 Oe at 30 kHz) for 30 s once the sample has been dc-field cooled to the destination temperature. The assisting ac field is then turned off and the measurement begins. A more mobile VLC,<sup>7</sup> that we call Sy, is obtained applying a symmetrical (sinusoidal) ac field (3.5 Oe and 30 kHz) for 30 s following the complete Asy protocol. The sinusoidal shaking field is turned off and the measurement begins. Linear Campbell regime was measured at an amplitude two orders of magnitude lower (0.04 Oe) and frequency 30 kHz.

### B. Campbell regime calculations

Pinning potentials corresponding to different VLCs were explored measuring the linear real penetration depth  $\lambda_R$  in the Campbell regime.<sup>23</sup> In a general case, the linear ac response is determined by the complex frequency dependent penetration depth  $\lambda_{ac}(f) = \lambda_R + i\lambda_I$ .<sup>24</sup> The function  $\chi(\lambda_{ac})$  depends on the sample geometry. To evaluate  $\lambda_{ac}$  we approximated our experimental geometry by a thin disk of radius  $R$  and thickness  $\delta$  in a transverse ac magnetic field. We used the numerical solution developed by Brandt,<sup>25,26</sup> in which  $\chi$  is determined by the adimensional parameter  $\lambda_{ac}/D$ , where  $D = (\delta R/2)^{1/2}$  is the characteristic length of the sample. In the Campbell regime the imaginary penetration depth  $\lambda_I \ll \lambda_R$  and dissipation is very small. This leads to a frequency independent  $\lambda_R = (\lambda_L^2 + \lambda_c^2)^{1/2}$ , where  $\lambda_L$  and  $\lambda_c = (\phi_0 B / 4\pi\alpha_L)^{1/2}$  are the London and Campbell penetration depths, respectively, and  $\alpha_L$  represents the curvature of the effective pinning potential well,<sup>24</sup> and  $\phi_0$  and  $B$  are the flux quantum and the magnetic induction. When the phase  $\varepsilon = \lambda_I/\lambda_R \ll 1$ , to first order in  $\varepsilon$ , we obtain

$$\chi' + i\chi'' = -1 + f(\lambda_R/D) + i\varepsilon g(\lambda_R/D), \quad (1)$$

where  $f$  and  $g$  are functions of the adimensional variable  $\lambda_R/D$ .<sup>25,26</sup> Therefore, in this limit, the inductive component of the ac susceptibility  $\chi'$  is determined by the experimental geometry and the adimensional parameter  $\lambda_R/D$  (for details of the numerical procedure see Ref. 26). The phase  $\varepsilon$  can be easily estimated from Eq. (1) and the experimental values of  $\chi'$  and  $\chi''$  as

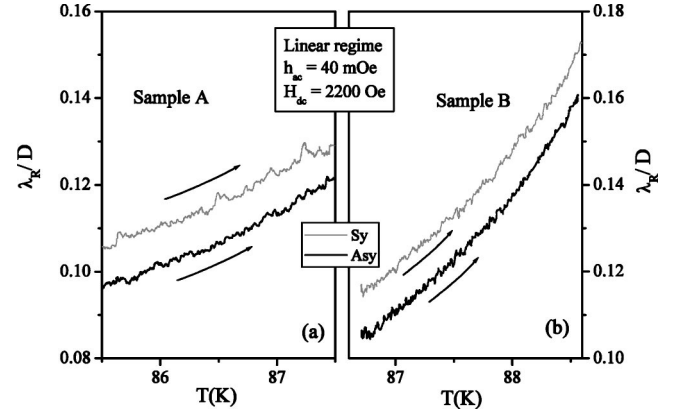


FIG. 1. Real linear penetration depth  $\lambda_R$ , normalized by the characteristic length  $D$  of the sample (see text) as a function of temperature in a warming process (arrows indicate temperature sweep direction), for YBCO crystals A (left) and B (right). Black (gray) curves start from an Asy (Sy) VLC (see text).  $H_{dc}$  was tilted  $20^\circ$  out of the twin planes.

$$\varepsilon = \frac{\chi''}{g\left(\frac{\lambda_R}{D}(\chi')\right)}. \quad (2)$$

## III. RESULTS AND DISCUSSION

Figure 1 compares curves for the real penetration depth  $\lambda_R/D$  as a function of temperature in a warming process starting from a Sy and an Asy VLC in two YBCO crystals, samples A and B. In both cases  $H_{dc}$  was tilted in  $\theta = 20^\circ$  away from the twin planes. In all the measured samples a clear difference in the penetration depth of both VLCs can be observed. It can be seen from Fig. 1 that, in that case, the initial relative difference  $[\lambda_R(\text{Sy}) - \lambda_R(\text{Asy})]/\lambda_R$  is around 9%. We note, however, that this value depends on the sample and the temperature where the protocols were carried out. To verify the validity of our experimental result, we carefully evaluated all the error sources in the  $\chi$  measurement (noise, signal phase, normalization procedure). Using an ac field of 40 mOe and 30 kHz, measurements displayed in Fig. 1, have an experimental precision better than  $\pm 1.3\%$ . We also checked that inversion of the first order approximation Eq. (1), is a very good estimation of  $\lambda_R$ : in our experimental penetration range, and for  $\varepsilon < 0.1$  a second order term modifies  $\lambda_R$  less than 0.8%. We note that in these evaluations, we take the model and the Brandt numerical procedure as exact. Obviously, to take into account the exact sample geometry would give different numerical values, but this fact would not affect the physics under discussion. Consequently, results in Fig. 1 show that oscillatory dynamics can directly modify the effective pinning potentials of vortices. It is clear that the VL is more pinned in the torn Asy than in the healed Sy VLC.

In Figs. 2(a) and 2(b) full curves of the linear ac susceptibility components  $\chi'(T)$  and  $\chi''(T)$  for sample B are shown. The small region of data used to plot Fig. 1 is encircled. A typical nonlinear  $\chi'(T)$  curve measured at a higher ac field

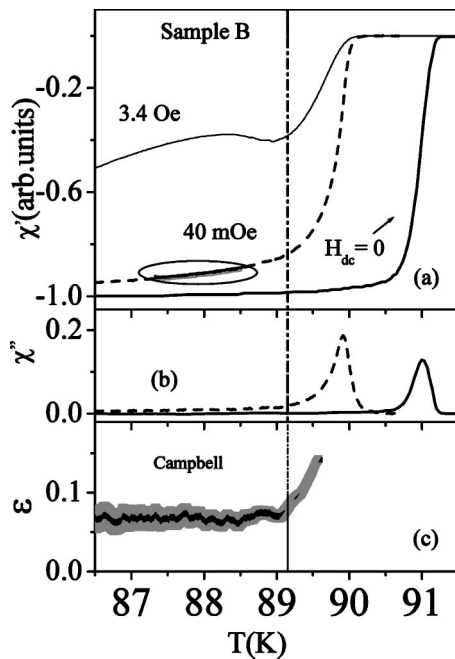


FIG. 2. Linear ac susceptibility components measured at 40 mOe (a)  $\chi'(T)$  and (b)  $\chi''(T)$  for  $H_{dc}=0$  (full line) and  $H_{dc}=2200$  Oe (dashed line) are shown. The encircled area indicates the region from where the data were extracted to calculate the curves in Fig. 1. A typical nonlinear  $\chi'(T)$  curve measured at a higher ac field with  $H_{dc}=2200$  Oe is shown. (c)  $\varepsilon=\lambda_I/\lambda_R$  obtained using Eq. (2) with its error is plotted (see text). Vertical line identifies the Campbell regime limit.

(3.4 Oe) displaying the typical peak effect is compared. The continuous line shows the zero field transition. Figure 2(c) shows the  $\varepsilon(T)$  curve and its experimental error obtained using Eq. (2). There is a constant phase  $\varepsilon\sim 0.07$ , until an upper temperature limiting the Campbell regime. This temperature for  $H_{dc}=2.2$  kOe is indicated in the figure with a vertical line. We also confirmed that below this temperature  $\chi'$  is frequency independent in the kHz range.

Complex dynamics deriving in striking features as memory effects appear in cases where there is a crucial competition between vortex-vortex interaction and random disorder. When strong correlated disorder prevails, none of these effects are present.<sup>6,8</sup> To check that the previous results effectively arise from complex dynamics, an analog experiment but with  $H_{dc}/c$  was made. Comparison between both experiments for sample A are summarized in Fig. 3. Measurements of  $\chi'+1$  at fixed temperature using different measuring ac fields after the Sy and Asy VLCs were prepared, are shown for  $H_{dc}/c(\theta=0^\circ)$  and  $\theta=20^\circ$ . The vertical dotted line indicates the limit of linear response. The corresponding values of  $\lambda_R/D$  were extracted from the Campbell response. As shown in Fig. 3, when the vortices are tilted away from the twin planes, two clearly different penetration depths result for the Sy and Asy VLCs, while when correlated pinning prevails, there is no evidence of distinct VLCs. This is an important result showing that complex oscillatory dynamics observed for  $\theta=20^\circ$  (and absent for small  $\theta$ ) in our previous work,<sup>7</sup> is related to these static VLCs.

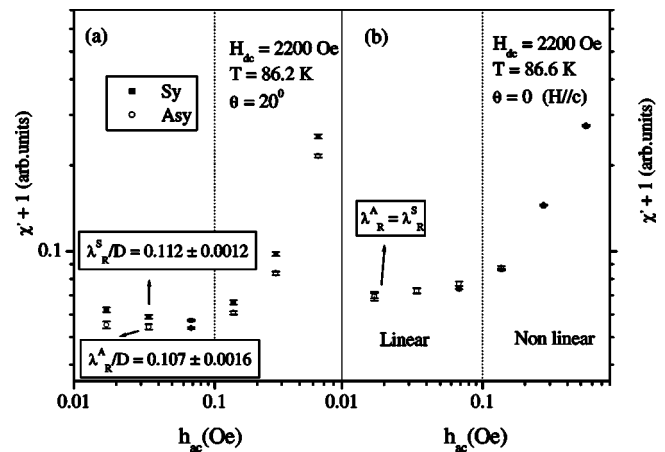


FIG. 3. ac permeability  $\chi'+1$  measured at different ac fields after the Sy and Asy VLCs were prepared, for two orientations between the dc field and twin boundaries: (a)  $\theta=20^\circ$  and (b)  $\theta=0^\circ$ . Vertical dotted lines indicate the limit of linear response. From the Campbell response shown in (a) two clearly different penetration depths result, while in (b) they are indistinguishable. Axes are shown in logarithmic scale.

Next, the stability of these different dynamic-modeled static VLCs was investigated. In Fig. 4 the evolution of  $\lambda_R/D$  during a very slow ( $\sim 2$  h) warming-cooling process W-C for the different VLCs is shown. In Fig. 4(a) the result of a W-C excursion of approximately 1.3 K after preparing the VL in the Sy and Asy VLCs at  $T\approx 87.3$  K are compared. It can be seen that the Sy VLC has an initial fast accommodation and after that it remains reversible for the whole measured temperature range. This initial relaxation is difficult to measure with a good temporal resolution, because of the large lock-in amplifier integration time required to detect such small signals. On the contrary, the more pinned Asy VLC relaxes slowly during the warming process. The difference in behavior is more clearly displayed in the inset, where the relative change of the penetration length  $\lambda_R(W)-(\lambda_R(C))/\lambda_R(W)$  as a function of temperature for both processes is compared. In Fig. 4(b) the Asy evolution is compared with that corresponding to a usual FC (ZF<sub>ac</sub>C) VLC. The FC VLC is practically reversible, although it seems to slightly relax towards the Sy curve. In fact, all the evolutions seem to get closer to a unique ac penetration depth.

We then performed a series of tests to investigate the nature of such a relaxation. An important result is that we observe the same final state after repeating the W-C process without applying the small measuring ac field. This suggests that the relaxation is due to a thermal activated process and it is supported by the fact that in an inverse cooling-warming process, beginning at the same temperature, no relaxation is observed. Note that the time scale of this relaxation process is larger than the time scale of vortex motion in Campbell response, contributing to negligible ac losses at 30 kHz.

As another test to confirm the thermal origin in the relaxation of the Asy VLC, we repeated the same procedure in another temperature range. In Fig. 5, evolutions of  $\lambda_R/D$  in similar W-C excursions are shown. In these cases, the Asy VLC was prepared at a lower temperature than in Fig. 4.

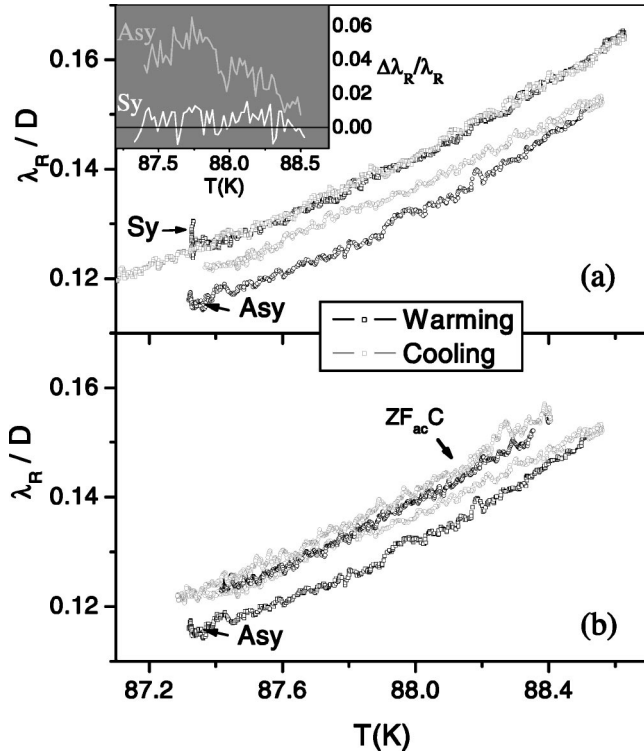


FIG. 4. Evolution of  $\lambda_R/D$  during a warming (black symbols) followed by a cooling (gray symbols) process, after preparing different VLCs: In (a) the evolution of Sy and Asy initial VLCs are shown. The Sy VLC has an initial fast accommodation after which it remains reversible for all the measured temperature range. The more pinned Asy VLC decays during the slow warming process. Inset: comparison of the relative change in  $\lambda_R$  for both starting VLCs (Sy in white, Asy in light gray). In (b) the evolution for the Asy initial VLC is compared with that corresponding to a ZF<sub>ac</sub>C VLC.

Vertical axes are shifted for clarity. In the upper curve (left axis), the sample was warmed to  $T_{\max}=87.5$  K and the response is reversible. However, if the same process is carried out up to a higher temperature (lower curve), the irreversibility reappears.

Before discussing the underlying physics that we believe explain our results, it is necessary to rule out an alternative explanation found in the recent literature for thermal relaxation in the Labusch constant. For example, in Ref. 27 a hysteretic linear response has been related with a remanent critical state profile. In that case, vortices perform small excursions around a point away from the bottom of the pinning potential well with a different curvature. Relaxation in the curvature is then associated to a thermal relaxation in the critical profile. Results shown in Fig. 3 rule out this explanation in the present case, because remanent profiles (if any) should be independent of the direction of the dc field. Additionally, if a critical profile relaxes, the vortex equilibrium position gradually shifts towards a higher curvature<sup>27</sup> (at the potential well minimum), contrary to what happens in the present case.

Let us now underline a possible scenario to explain the above results: Campbell regime is characterized by a very small dissipation that may be mainly due to small thermal

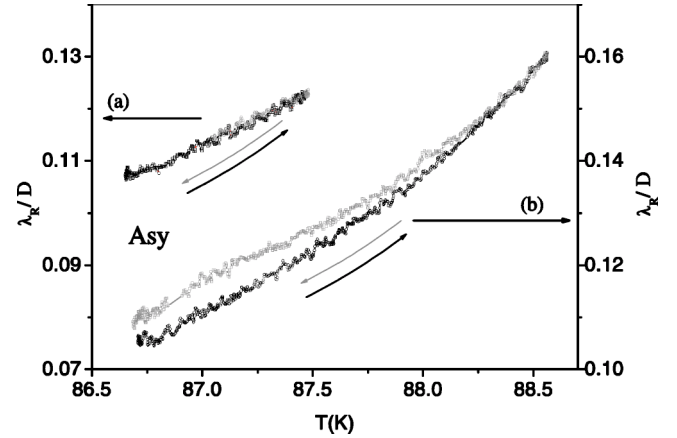


FIG. 5. (a) Left axis: Evolution of  $\lambda_R/D$  in a similar procedure than that shown in Fig. 4 for the Asy VLC, but for a lower temperature range. The response is reversible. (b) Right axis: The same process carried up to a higher temperature: irreversibility emerges. Vertical axis scales are shifted for clarity.

creep.<sup>24</sup> In that case ac losses are very small because the characteristic time scale for creep is much larger than the ac field period. Consequently, the VL is observed to slowly adapt to a more stable (or less stressed) VLC.

Numerical simulations recently confirmed that the more mobile Sy VLC is more ordered, while the less mobile Asy VLC is characterized by a greater number of topological defects or dislocations.<sup>20</sup> On the other hand, recent theoretical work<sup>28</sup> has predicted that plastic vortex creep, in a dislocated vortex solid, would have higher exponents for the power-law divergence of the creep barriers than elastic vortex creep occurring in an elastic medium free of topological defects.

In this framework, the fast initial relaxation in the Sy VLC could be associated to a small elastic creep where vortices only slightly adapt better to the pinning potential without modifying the structure of the VL. On the contrary, the slow thermal relaxation in the torn Asy VLC can be due to plastic creep, where the number of dislocations is being reduced and the system evolves towards a less strained (and less pinned) configuration. It seems that the protocol that creates the Asy VLC promotes more dislocations than the existing number in the stable configuration.

Finally, as a result of thermal annealing, all the prepared VLCs seem to relax to final static VLCs with a degree of pinning similar to the one observed for the initial Sy VLC. This result can be surprising, because warming curves reached temperatures above the onset of the PE (see Fig. 2) where a more disordered (and more pinned) VL is expected. However, the observed behavior is consistent with the inexistence of the PE in the linear regime. In Fig. 2 it can be seen that while the PE is clearly displayed in the nonlinear response (associated with the measured  $J_c$ ), it is absent in the  $T$  dependence of the Labusch constant. We think that this fact is crucial for the understanding of the nature of the peak effect in YBCO crystals.

#### IV. CONCLUSIONS

We have presented linear ac susceptibility results in twinned YBCO crystals that show that the solid vortex lat-

tice, in the vicinity of the peak effect, is organized by its oscillatory dynamical history in different vortex lattice configurations VLCs characterized by different effective pinning potential curvature. The obtained Labusch parameter  $\alpha_L$  for the VLC healed by the application of a sinusoidal ac magnetic field is smaller than the obtained parameter for a torn defective one (torn by the application of a sawtooth ac magnetic field). This result would lead us to describe the less mobile<sup>7,13</sup> torn lattice as more pinned. We point out, however, that there is not a trivial relationship between vortex lattice mobility and pinning potential curvature,  $\alpha_L$ , particularly near the PE region.

We have also found that, interestingly, the more pinned torn vortex lattice is unstable and relaxes without assistance of macroscopic forces towards a more ordered lattice with a smaller Labusch parameter. We conclude that a large density of defects increases the effective pinning potential curvature

and inhibits vortex mobility, contrary to the effect of a small density of topological defects. However, there seems to be a temperature dependent equilibrium density of defects towards which the more pinned and more ordered lattices relax showing different relaxation time scales probably related to fast elastic and slow plastic creep process. There still remains the need to determine how general these results are, exploring YBCO crystals with controlled defects and other superconducting materials that show peak effect.

#### ACKNOWLEDGMENTS

We thank S. O. Valenzuela and A. Moreno for useful discussions and C. Chliotte for technical support. This work was partially supported by UBACyT X071, CONICET PIP 4634.

\*Electronic address: pasquini@df.uba.ar

- <sup>1</sup>G. Blatter, M. V. Feigel'man, V. B. Geshkenbein, A. I. Larkin, and V. M. Vinokur, *Rev. Mod. Phys.* **66**, 1125 (1994); E. H. Brandt, *Rep. Prog. Phys.* **58**, 1465 (1995).
- <sup>2</sup>T. Nattermann and S. Scheidl, *Adv. Phys.* **49**, 607 (2000).
- <sup>3</sup>W. De Sorbo, *Rev. Mod. Phys.* **36**, 90 (1964).
- <sup>4</sup>See, for example, W. Henderson, E. Y. Andrei, and M. J. Higgins, *Phys. Rev. Lett.* **81**, 2352 (1998); Z. L. Xiao, E. Y. Andrei, and M. J. Higgins, *ibid.* **83**, 1664 (1999).
- <sup>5</sup>Y. Paltiel, D. T. Fuchs, E. Zeldov, Y. N. Myasoedov, H. Shtrikman, M. L. Rappaport, and E. Y. Andrei, *Phys. Rev. B* **58**, R14 763 (1998); Y. Paltiel, E. Zeldov, Y. N. Myasoedov, H. Shtrikman, S. Bhattacharya, M. J. Higgins, Z. L. Xiao, E. Y. Andrei, P. L. Gammel, and D. J. Bishop, *Nature (London)* **403**, 398 (2000).
- <sup>6</sup>S. O. Valenzuela and V. Bekeris, *Phys. Rev. Lett.* **84**, 4200 (2000); S. O. Valenzuela, B. Maiorov, E. Osquiguil, and V. Bekeris, *Phys. Rev. B* **65**, 060504(R) (2002).
- <sup>7</sup>S. O. Valenzuela and V. Bekeris, *Phys. Rev. Lett.* **86**, 504 (2001).
- <sup>8</sup>S. Kokkaliaris, A. A. Zhukov, P. A. J. de Groot, R. Gagnon, L. Taillefer, and T. Wolf, *Phys. Rev. B* **61**, 3655 (2001).
- <sup>9</sup>D. Stamopoulos, M. Pissas, and A. Bondarenko, *Phys. Rev. B* **66**, 214521 (2002).
- <sup>10</sup>N. Chikumoto, M. Konczykowski, N. Motohira, and A. P. Malozemoff, *Phys. Rev. Lett.* **69**, 1260 (1992); D. T. Fuchs, E. Zeldov, M. Rappaport, T. Tamegai, S. Ooi, and H. Shtrikman, *Nature (London)* **391**, 373 (1998).
- <sup>11</sup>R. B. Flippen, T. R. Askew, J. A. Fendrich, and C. J. van der Beek, *Phys. Rev. B* **52**, R9882 (1995).
- <sup>12</sup>A. Pautrat, C. Goupil, C. Simon, N. Lütke-Entrup, B. Plaçais, P. Mathieu, Y. Simon, A. Rykov, and S. Tajima, *Phys. Rev. B* **63**, 054503 (2001).
- <sup>13</sup>S. O. Valenzuela and V. Bekeris, *Phys. Rev. B* **65**, 134513 (2002).
- <sup>14</sup>G. P. Mikitik and E. H. Brandt, *Phys. Rev. B* **69**, 134521 (2004).
- <sup>15</sup>X. S. Ling, S. R. Park, B. A. McClain, S. M. Choi, D. C. Dender, and J. W. Lynn, *Phys. Rev. Lett.* **86**, 712 (2001).
- <sup>16</sup>P. Chaddah, *Phys. Rev. B* **62**, 5361 (2000).
- <sup>17</sup>A. Moreno, S. O. Valenzuela, G. Pasquini, and V. Bekeris, *Physica C* **408-410**, 571 (2000).
- <sup>18</sup>I. V. Aleksandrov, A. B. Bykov, I. P. Zibrov, I. N. Makarenko, O. K. Mel'nikov, V. N. Molchanov, L. A. Muradyan, D. V. Nikiforov, L. E. Svistov, V. I. Simonov, S. M. Chigishov, A. Ya. Shapiro, and S. M. Stishov, *JETP Lett.* **48**, 493 (1988).
- <sup>19</sup>M. J. Higgins and S. Bhattacharya, *Physica C* **257**, 232 (1996), and references therein.
- <sup>20</sup>S. O. Valenzuela, *Phys. Rev. Lett.* **88**, 247003 (2002).
- <sup>21</sup>V. F. Correa, G. Nieva, and F. de la Cruz, *Phys. Rev. Lett.* **87**, 057003 (2001).
- <sup>22</sup>G. Pasquini, V. Bekeris, A. Moreno, and S. O. Valenzuela, *Physica C* **408-410**, 591 (2004).
- <sup>23</sup>A. M. Campbell, *J. Phys. C* **4**, 3186 (1971); E. H. Brandt, *Phys. Rev. Lett.* **67**, 2219 (1991); *Physica C* **195**, 1 (1992).
- <sup>24</sup>C. J. van der Beek, V. B. Geshkenbein, and V. M. Vinokur, *Phys. Rev. B* **48**, 3393 (1993); M. W. Coffey and J. R. Clem, *ibid.* **45**, 9872 (1992).
- <sup>25</sup>E. H. Brandt, *Phys. Rev. B* **50**, 13 833 (1994).
- <sup>26</sup>G. Pasquini, L. Civale, P. Levy, H. Lanza, and G. Nieva, *Physica C* **274**, 165 (1997); G. Pasquini, L. Civale, H. Lanza, and G. Nieva, *Phys. Rev. B* **59**, 9627 (1999).
- <sup>27</sup>R. Prozorov, R. W. Giannetta, N. Kameda, T. Tamegai, J. A. Schlueter, and P. Fournier, *Phys. Rev. B* **67**, 184501 (2003).
- <sup>28</sup>A. van Otterlo, R. T. Scalettar, G. T. Zimanyi, R. Olsson, A. Petrean, W. Kwok, and V. Vinokur, *Phys. Rev. Lett.* **84**, 2493 (2000); J. Kierfeld, H. Nordborg, and V. M. Vinokur, *ibid.* **85**, 4948 (2000).